Effects of Hydration on Mechanical Properties of a Highly Sclerotized Tissue

Dana N. Moses,* Michael G. Pontin,† J. Herbert Waite,* and Frank W. Zok†
*Marine Science Institute and †Materials Department, University of California, Santa Barbara, California 93106

ABSTRACT The jaws of the bloodworm *Glycera dibranchiata* consist principally of protein and melanin scaffolds with small amounts of unmineralized copper (Cu) and mineralized atacamite ($Cu_2Cl(OH)_3$) fibers in distinct regions. Remarkably, when tested in air, the regions containing unmineralized Cu are the hardest, stiffest, and most abrasion resistant. To establish the functions of jaw constituents in physiologically relevant environments, this study examines the effects of hydration on their response to indentation, scratching, and wear. Although all jaw regions are degraded by the presence of water, the ones containing unmineralized Cu are affected least. Notably, scratch depths in the bulk and the atacamite-containing regions double when wet, whereas the corresponding increase in the regions with unmineralized Cu is ~20%. The results support the view that Cu ions are involved in the formation of intermolecular coordination complexes, creating a cross-linked molecular network that is both mechanically robust and resistant to water ingress. Hydration effects are greatest during wear testing, rates of material removal in water being about three times those in air. The mechanism underlying accelerated wear is suspected to involve coupled effects of near-surface damage and enhanced water ingress, resulting in increased plasticization and susceptibility to plastic plowing.

INTRODUCTION

Nature uses a limited molecular repertoire to build robust biomaterials, adjusting hardness, stiffness, and toughness in combinations that reflect adaptive function and fulfill the requirements of a natural material. There are myriad examples of robust materials throughout nature worth studying to improve our understanding of the functions and designs of these materials (1).

The marine bloodworm *Glycera* (Fig. 1) is a raptor that is itself hunted by a wide range of predators including humans. By spending most of its life burrowing through benthic sand or mud, the worm remains concealed from its predators. Benthic concealment, however, also enhances *Glycera*'s own hunting strategy—the surprise attack. *Glycera* waits just below the sediment surface for a passing amphipod or another worm. During attack, the proboscis, an eversible extension of the pharynx, rapidly erupts from the head of the worm to immobilize and engulf the prey. The tip of the everted proboscis is armed with four hard and stiff jaws that serve both as graspers and as hypodermic needles. As graspers, the jaws firmly grip and hold the prey, and, as needles, they penetrate its integument and inject paralyzing venom (2,3). The jaws must be hard and stiff enough to penetrate the prey, the carapace of a small crustacean, for example, but must also withstand the bending forces involved in the grasping action. Further, as an intertidal dweller, most of *Glycera*'s meals come with sand particles, so its jaws need to be highly wear resistant as well.

Overall, *Glycera* jaws are composed of ~40 wt % protein, 40 wt % melanin, and <10 wt % metals and minerals (4), the latter mostly in the form of unmineralized copper (Cu) (5) with small amounts of mineralized atacamite ($Cu_2Cl(OH)_3$) fibers (6). The Cu in all forms is concentrated at the tip of the jaw, typically within ~30 μm of the surface (5). Additionally, the jaw protein is very glycine and histidine rich (4,7).

Interest in the mechanical properties of *Glycera* jaws was sparked when nanoindentation tests revealed that the hardness, H, and Young's modulus, E, as well as the metric H^3/E^2 (an indicator of abrasion resistance in ceramics (8)) were highest in the near-tip, near surface regions of the jaw (6). Because the atacamite fibers are located in essentially the same regions, the enhancement in properties was initially (incorrectly) attributed to the mineral. Clarification came in a subsequent study (9) in which nanoindentation measurements were augmented with fine-scale scratch and wear tests. The latter showed that, in fact, the Cu-rich regions of the jaw tip are comprised of three distinct microstructural domains (not simply one atacamite-containing layer), each with a thickness of order 3–20 μm (Fig. 1 *d*). The surface layer (denoted *A*) contains unmineralized Cu but is devoid of atacamite. Beneath it is a layer (*B*) containing atacamite, followed by second layer (*C*) containing unmineralized Cu, all overlying the metal-free bulk of the jaw (*D*). Interestingly, when the jaws are dry, the two layers containing the unmineralized Cu are harder, stiffer, and more wear-resistant than those containing atacamite (9).

The principal objective of the study presented here is to assess the effects of hydration on the property variations in the near-tip regions of the *Glycera* jaws. The work is motivated in part by the recognition that *Glycera* lives in benthic sediments so the jaws are naturally exposed to seawater. Additionally,

Submitted August 28, 2007, and accepted for publication December 3, 2007.
Dana N. Moses and Michael G. Pontin contributed equally to this work.
Address reprint requests to Dana N. Moses, E-mail: moses@lifesci.ucsb.edu.
Editor: Elliot L. Elson.

0006-3495/08/04/3266/07 $2.00
doi: 10.1529/biophysj.107.120790

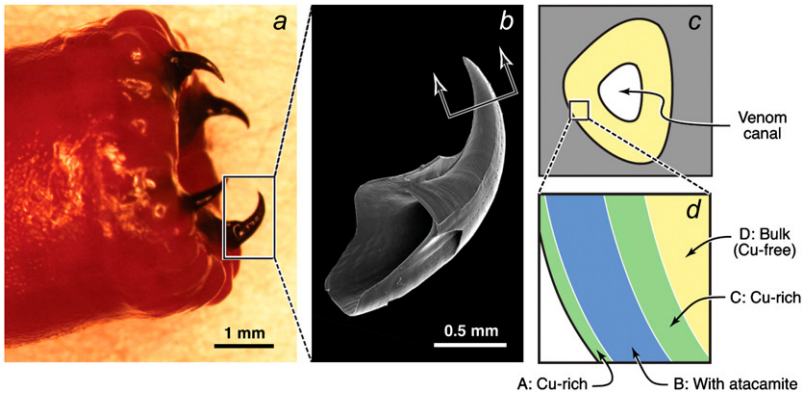

FIGURE 1 Overview of the jaw structure: (*a*) photograph of a worm head, showing the four eversible jaws; (*b*) a single extracted jaw, imaged in a scanning electron microscope; (*c*) schematic of transverse cross section near the jaw tip, along the line shown in *b*; and (*d*) schematic of the four compositional domains in the near surface regions.

because studies of this type have possible implications for biomimetic material design (for applications in dental and orthopedic restorations, for example), the pertinent structure-function relationships are those in the hydrated state. A secondary objective is to assess the utility of scratch testing as a means of continuous property measurement in graded and/or layered structures. Success on this front may have important implications for the way in which biological materials are characterized in the future.

EXPERIMENTAL PROCEDURES

Glycera dibranchiata worms were ordered live from Maine Bait Company (Newcastle, ME). Batches of worms were frozen at −80°C for ~1 h and then thawed and dissected for jaws. The dissected jaws were washed for 24 h in multiple changes of milliQ water, and any remaining tissue was then removed with microforceps.

Clean, dry jaws were embedded in an epoxy (EMBed 812, Electron Microscopy Sciences, Hatfield, PA) mixed according to the manufacturer's specifications. The epoxy was cured for ~12 h at 70°C. Embedded jaws were sectioned on an ultramicrotome, and the block faces of the exposed samples were used for mechanical testing. Some of the thin microtomed sections were transferred onto Cu grids and subsequently examined in a JEOL 2000FX transmission electron microscope (TEM).

Indentation, scratch, and wear tests were conducted using a fully automated nanomechanical test system capable of normal and lateral loading (TriboIndenter, Hysitron, Minneapolis, MN). Samples were placed in a small crucible to facilitate sample hydration. All tests were performed at room temperature with a diamond indenter with a 1-μm tip radius. Scanning probe microscopy (SPM) images were obtained before and after each test using the same indenter. Once a series of tests in ambient air was complete, the crucible was filled with distilled water to several millimeters above the sample surface. Following a hydration period of ~12 h, the tests were repeated in regions close to those tested dry.

Indentation tests were performed in each of the four microstructural domains. The peak load was 500 μN, with loading and unloading rates of 100 μN/s and a 60-s hold at peak load. Hardness and modulus were calculated from the unloading portions of the load-displacement curves following standard analysis procedures (10).

Scratch tests were performed perpendicular to the layer boundaries, from the bulk of the jaw toward the epoxy. Individual scratches typically passed through several layers. The test protocol consisted of 1), applying a normal load in the range of 250–2000 μN at a rate of 100 μN/s; 2), holding at peak load for 5 s; 3), displacing the indenter laterally over a distance of 15 μm at a rate of 0.33 μm/s; 4), holding for 5 s; and 5), unloading at 100 μN/s. Continuous measurements were made of normal and lateral forces, F_N and F_L, as well as the corresponding displacements, δ_N and δ_L. Material response was characterized principally by the normalized force, $F_L/F_N^{\S}$, ([§]For purely elastic contact, $F_L/F_N = \mu$ where μ is the Coulomb friction coefficient.) and the normalized scratch depth, $\delta_N R/F_N$. (In the fully plastic indentation regime, $\delta_N R/F_N$ asymptotically approaches a constant value, inversely proportional to hardness, H.)

Wear tests were performed by rastering the indenter over the surface via the SPM imaging mode of the test system. Each test consisted of 4–10 scans over an area 20 μm × 20 μm at a rate of 60 μm/s under a normal load of 500 μN. Wear depths were ascertained from low-load (2 μN) SPM scans performed before and after each test. The latter scans covered an area 50 μm × 50 μm, encompassing the entire worn area as well as a band of pristine material around its perimeter. Such tests were performed in both dry and wet conditions, with the two regions within 100 μm of one another.

RESULTS

Indentation

Measurements of hardness and modulus, both dry and hydrated, for a representative jaw sample are shown in Fig. 2 along with an SPM image of the tested region. The key observations follow.

1. The regions containing unmineralized Cu (A and C) are the hardest and the stiffest, both wet and dry. Moreover, their properties are essentially indistinguishable from one another.
2. Despite the presence of atacamite fibers in region B, its hardness and modulus are comparable to those of the bulk material.
3. When hydrated, regions A and C exhibit reductions in E and H of ~20% relative to the values obtained dry. In contrast, the corresponding property reductions in B and D are greater, typically ~40%.

Scratch resistance

Variations in the normalized scratch force, F_L/F_N, with position are plotted in Fig. 3. The trends are qualitatively consistent with those obtained from the indentation tests. That is, regions A and C exhibit properties similar to one another, both wet and dry. Hydration causes a 20–25% elevation in

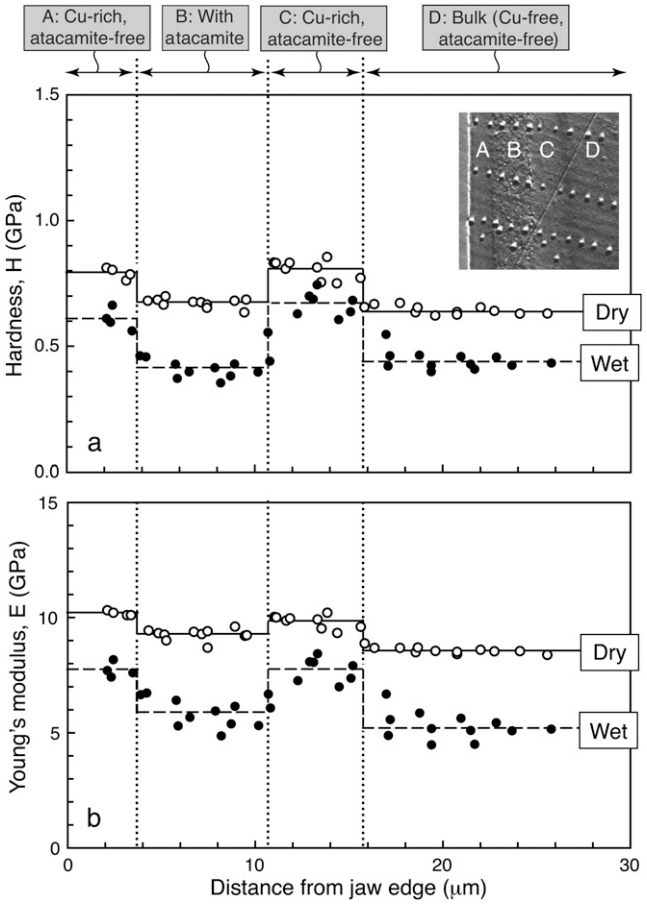

FIGURE 2 (*a*) Hardness and (*b*) Young's modulus within the jaw layers, measured by nanoindentation. An SPM image of a portion of the indented region is inset. Also shown are layer boundaries (*vertical lines*) and average property values within each layer (*horizontal lines*).

the average scratch forces in these regions, from ~0.37 to 0.45. Additionally, regions B and D exhibit comparable properties to one another, with slightly higher (~30%) elevations in scratch force on hydration, from 0.42 to 0.55.

Results from scratch tests performed over the load range $F_N = 250-2000\,\mu$N and extending through the four layers of several jaw samples are summarized in Fig. 4. Presentation of the results is guided by a mechanics model of plowing with a hard spherical indenter across a flat block of a perfectly plastic medium (Appendix). The model yields a predicted scratch force given by

$$\frac{F_L}{F_N} = \mu + \beta\sqrt{\frac{F_N}{R^2H}}, \tag{1}$$

where μ is the Coulomb friction coefficient (that is, F_L/F_N for purely elastic contact), and β is a nondimensional coefficient. Accordingly, the results in Fig. 4 are presented as F_L/F_N versus $\sqrt{F_N/R^2H}$, with H taken as the average value within the respective layer measured by indentation (Fig. 2). Each point shown is the mean of multiple measurements. A

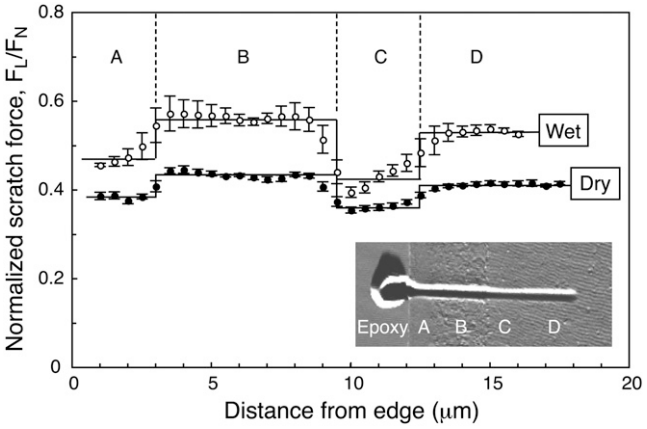

FIGURE 3 Normalized scratch forces across the four microstructural domains. Each datum represents the mean of measurements collected within a 0.5-μm increment of lateral displacement, from three independent scratches, all performed on a single jaw sample with a peak normal force $F_N = 500\,\mu$N. An SPM image of one scratched region is inset. Also shown are layer boundaries and average property values within each layer. Error bars represent 1 SD from the mean.

linear regression analysis of the data for dry scratches yields $\mu = 0.22 \pm 0.01$, in good agreement with the value reported previously (9) (0.23 ± 0.02). Similar analysis of the measurements made in the wet condition yields $\mu = 0.27 \pm 0.02$. Further statistical analysis of the data indicates that the individual layers do not exhibit significantly different friction coefficients but that the difference in the dry and wet values is indeed statistically significant (within 95% confidence level). Additionally, the value of β is essentially the same in dry and wet conditions ($\beta \approx 0.25$).

Confirmation of the preceding rankings was obtained from measurements of the displacement, $\delta_N R/F_N$, plotted in Fig. 5. Under both dry and wet conditions, the regions rich in unmineralized Cu (A and C) emerge as the most scratch resistant. When a region is wet, the scratch depth increases by a factor of ~2 in regions B and D and by only ~20% in A and C.

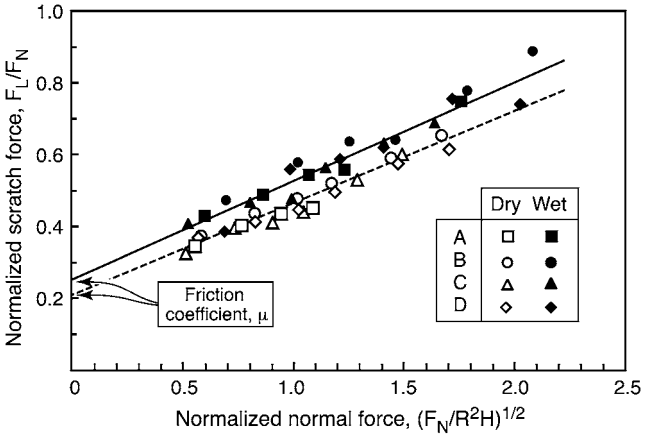

FIGURE 4 Compilation of scratch force measurements in the four regions over a load range $F_N = 250$–$2000\,\mu$N, both dry and wet.

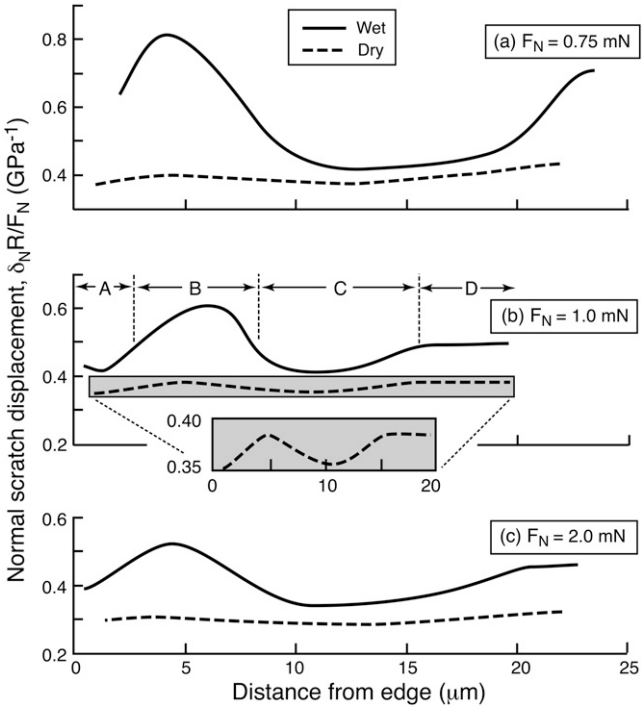

FIGURE 5 Normal scratch displacements across the layers, obtained from representative scratches at various normal forces.

Wear resistance

Results from representative dry and wet wear tests as well as a TEM image of a neighboring region are summarized in Fig. 6. The TEM image confirms the presence of atacamite fibers in region B as well as the adjacent mineral-free layers (A in upper left and C in lower right). Energy dispersion x-ray spectroscopy maps of Cu and Cl (not shown) corroborate the layer assignments: only Cu is present in A and C, both Cu and Cl are in B (consistent with the composition of atacamite), and neither Cu nor Cl is in D. Average wear depths within each region obtained from four dry and four wet tests on a single jaw sample are summarized in Fig. 7. The atacamite-containing region clearly exhibits the greatest wear depth. Furthermore, when the sample is wet, the wear rates increase by a factor of ~3 in all regions. The variations in wear from one location to the next preclude a quantitative assessment of the effects of water on the wear resistance of the various microstructural domains.

The variations in wear rates are further exemplified by test results on different jaw samples (Fig. 8). Here, the wear rates in a given domain vary by as much as a factor of two. However, within each sample, the wear rate in layer B is always about twice that in layers A and C, consistent with the averages of multiple measurements on a single sample (Fig. 7).

DISCUSSION

Unmineralized Cu plays a key role in the hardness and the stiffness of the near-tip regions of the *Glycera* jaw. The elevations in these properties are manifested in lower scratch force and normal displacement during scratch testing. One inference is that the Cu interacts with the constituent histidine-rich proteins and melanin in forming intermolecular cross-links (4). Indeed, both histidine and melanin are known to bind Cu tightly. For instance, *Sepia* melanin (a standard eumelanin) binds Cu 30 times more tightly at pH 5.8 than EDTA (11), a common chelator.

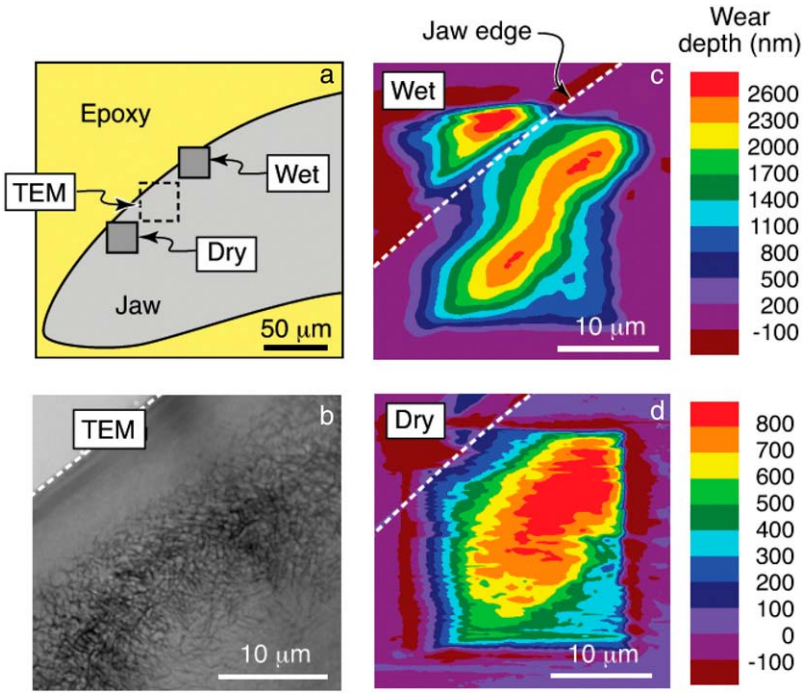

FIGURE 6 Representative wear results from one jaw sample. (*a*) Schematic of the jaw cross section and test locations. (*b*) TEM image showing atacamite fibers in layer B as well as the adjacent mineral-free regions, A and C. (*c* and *d*) Wear depth maps from dry and wet tests, obtained from SPM images.

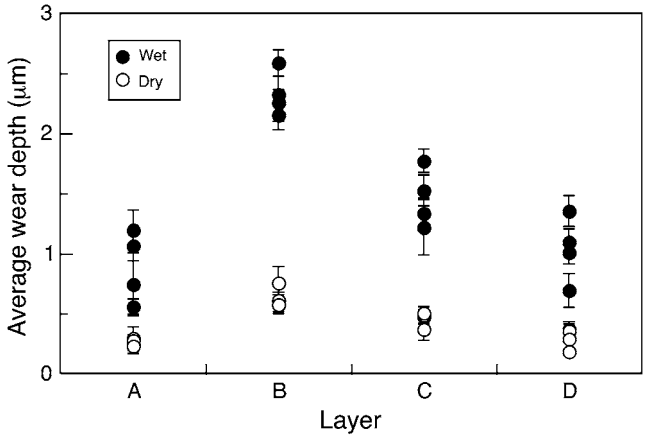

FIGURE 7 Summary of wear depths from multiple tests within a single jaw sample. Each test consisted of 10 wear passes. Error bars represent 1 SD from the mean.

The unmineralized Cu also appears to attenuate the effects of hydration on mechanical properties. In both the jaw bulk and the atacamite-containing regions, the hardness in water is ~40% lower than that measured in air, presumably as a result of the plasticization of the organic material by water. In contrast, the corresponding reduction in the regions containing unmineralized Cu is only ~20%. Differences in scratch depth caused by water are even greater, the depths typically increasing ~100% in the bulk and only ~20% in regions with unmineralized Cu. The reduced susceptibility of the latter region to degradation is likely caused by reduced diffusivity and solubility of water in the organic matrix in the presence of Cu. The effect may be physical in nature, with the Cu ions occupying intermolecular sites that would otherwise

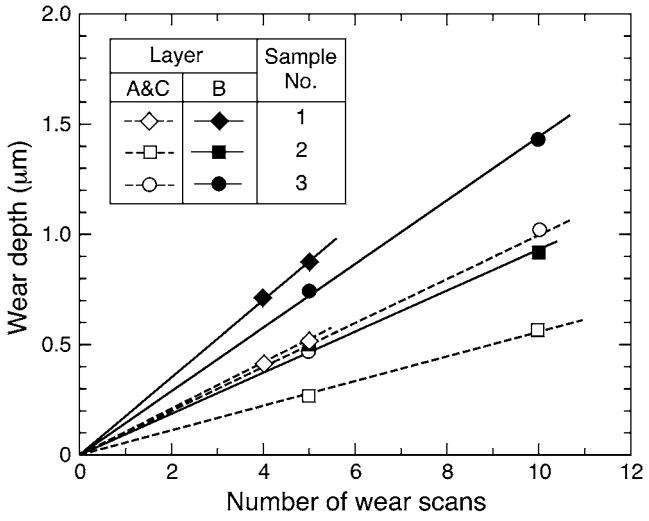

FIGURE 8 Variations in wear depth with number of wear scans for three hydrated jaw samples. The results illustrate the property variations among jaws as well as the essentially fixed ratio of wear rates in the atacamite-containing region and those with unmineralized Cu.

be available for occupation by water molecules. The intermolecular cross-links formed by the Cu-histidine complexes may also contribute to the suppression of water ingress.

Further inferences might be made regarding jaw synthesis. One intriguing hypothesis is that the organic melanin matrix is the same throughout the jaw but that the histidine-rich protein is selectively localized to the near-surface regions of the jaw tip, causing Cu to be directed to those areas. Furthermore, the presence of subsurface Cl may lead to the formation of atacamite fibers (in layer B) and hence to depletion of unmineralized Cu. The latter reduces the degree of cross-linking, causing the organic matrix within this layer to be softer, more compliant, and more susceptible to mechanical property changes with hydration than the surrounding Cu-rich layers.

The scratch force measurements can be rationalized in terms of material hardness and interfacial friction. Specifically, an analysis of plastic plowing indicates that the normalized scratch force F_L/F_N varies linearly with both the friction coefficient m and the root of the normalized normal force F_N/R^2H. The implication is that the scratch test can be used as a continuous measurement method to infer the fundamental tribological properties of finely layered and/or graded structures. It may find particular utility in probing dentin-enamel and cementum-dentin junctions in human teeth (12–15), the bone-cartilage interface (16,17), mussel byssus (18), insect mandibles (19), and jaws and teeth of various marine animals (18,20,21).

The effect of atacamite fibers on wear rate is broadly consistent with previous studies on polymer matrix materials, wherein additions of hard particles or fibers lead to increased wear. The elastic/plastic mismatch between the phases and the low toughness of the reinforcements promote cracking and chipping of the reinforcements and increase the propensity for plastic deformation and damage within the matrix (22–24). These correlations are in accord with the twofold increase in wear rate of the atacamite-containing region of the jaw tip relative to the surrounding (unmineralized) regions.

The results presented in this study raise questions about nature's adaptive role for the atacamite fibers. Clearly, they do not improve wear resistance of the jaw surfaces. The fact that the fibers are oriented parallel to the jaw surface and located near (but not at) the surface suggests that their role is to provide increased bending stiffness and strength. This proposed function remains to be tested.

The mechanism by which water accelerates wear remains unknown. Clearly, the magnitude of this effect (~3-fold) is much greater than those on the hardness or the modulus. One possibility is that near-surface damage produced during one wear cycle promotes water ingress; the resulting plasticization renders the material more susceptible to plastic plowing and further damage during subsequent wear cycles. The coupling between wear damage and plasticization would be expected to yield larger effects for repeated loadings (as in the wear tests) than those obtained during a single loading cycle (via indentation or scratching).

CONCLUSIONS

The near-surface regions containing unmineralized Cu are the hardest and stiffest of the jaw tip, both wet and dry. More importantly, these regions appear to be the least susceptible to degradation by water, as manifested in both indentation and scratch resistance. These trends implicate the interactions between the unmineralized Cu and the organic matrix material—an intricate blend of eumelanin and histidine-rich proteins—as critical to the mechanical robustness of the jaws.

The scratch test provides valuable information about the mechanical properties of systems with finely graded or layered structures. Its main advantage over indentation is that it enables continuous property measurement over a specified region. The test can be performed readily in water or other liquid media, thereby yielding insights into the functions of biological materials in physiologically relevant environments. Further analysis pertinent to the interpretation of scratch measurements is the focus of ongoing investigations.

APPENDIX: ANALYSIS OF PLOWING THROUGH A PLASTIC MEDIUM

Here we outline a mechanics model of the scratch test as it applies to our measurements. The assumed scratch geometry is depicted in Fig. 9. A hard spherical indenter of radius R is pushed into a rigid, perfectly plastic material with a normal force, F_N, yielding a circular indentation of radius

$$a = \sqrt{2Ru_o}, \tag{A1}$$

where u_o is the maximum penetration depth. The indenter is then moved laterally in the x-direction, plowing through the underlying material. The scratch depth is assumed to be equal to the initial indentation depth after application of F_N. The lateral force needed to produce the scratch is obtained from an analysis based on the principle of virtual work.

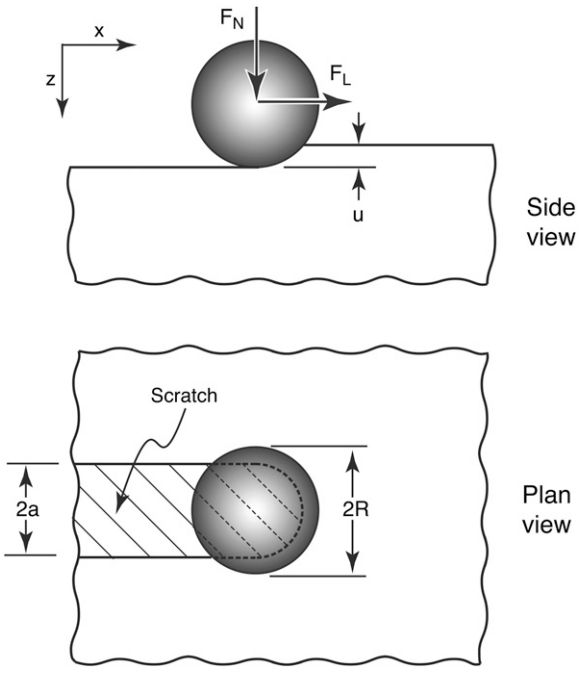

FIGURE 9 Schematic of the scratching process.

Once scratching has achieved steady state, with a scratch length greater than the contact radius, the rates of plastic dissipation, dW_p/dx, and frictional dissipation, dW_f/dx, reach constant values. Their sum is set equal to the rate of work done by the scratch force, notably $dW/dx = F_L$. If sliding at the interface between the two bodies obeys Coulomb's law with friction coefficient μ, the frictional dissipation is simply $dW_f/dx = \mu F_N$.

The rate of plastic dissipation is obtained from an analysis of an elemental strip of width dx during formation of a cylindrical divot of width $2a$, length dx, and depth u_o by a cylindrical indenter of radius R. The result can be expressed formally as

$$\frac{dW_p}{dx} = \int_o^{u_o} f_N(u)du, \tag{A2}$$

where $f_N(u)$ is the force per unit length of cylinder, given by

$$f_N(u) = 2a\sigma_y k_1 = 2\sqrt{2Ru}\,\sigma_y k_1, \tag{A3}$$

with k_1 being a plastic constraint factor (of order unity). Combining Eqs. A1–A3 and integrating yields,

$$\frac{dW_p}{dx} = \frac{2\sigma_y k_1 a^3}{3R}, \tag{A4}$$

with the contact radius related to the normal force through $F_N = k_2\pi a^2\sigma_y$, $k_2 \approx 3$, and the hardness $H \approx 3\sigma_y$, the plastic dissipation rate becomes

$$\frac{dW_p}{dx} = \frac{2k_1}{9\pi^{3/2}}\sqrt{\frac{F_N^3}{R^2H}}. \tag{A5}$$

Finally, setting the sum of the plastic and frictional dissipation rates equal to the actual work rate gives the normalized scratch force

$$\frac{F_L}{F_N} = \mu + \frac{2k_1}{9\pi^{3/2}}\sqrt{\frac{F_N}{R^2H}}. \tag{A6}$$

This result is equivalent to Eq. 1 in the text with $\beta \equiv 2k_1/9\pi^{3/2}$.

The authors gratefully acknowledge financial support from the National Institutes of Health (NIHR01DE014672).

REFERENCES

1. Currey, J. D. 1999. The design of mineralised hard tissues for their mechanical functions. *J. Exp. Biol.* 202:3285–3294.
2. Michel, C. 1970. Physiological role of the proboscis of four polychaete annelids belonging to the genera: *Eulalia, Phyllodoce, Glycera*, and *Notomastus*. *Cah. Biol. Mar.* 11:209–228.
3. Meunier, F. A., Z.-P. Feng, J. Molgo, G. W. Zamponi, and G. Schiavo. 2002. Glycerotoxin from *Glycera convoluta* stimulates neurosecretion by up-regulating N-type Ca^{2+} channel activity. *EMBO J.* 21:6733–6743.
4. Moses, D. N., J. H. Harreld, G. D. Stucky, and J. H. Waite. 2006. Melanin and *Glycera* jaws: emerging dark side of a robust biocomposite structure. *J. Biol. Chem.* 281:34826–34832.
5. Gibbs, P. E., and G. W. Bryan. 1980. Cu—the major metal component of Glycerid polychaete jaws. *J. Mar. Biolog. Assoc. U. K.* 60:205–214.
6. Lichtenegger, H. C., T. Schöberl, M. H. Bartl, J. H. Waite, and G. D. Stucky. 2002. High abrasion resistance with sparse mineralization: Cu biomineral in worm jaws. *Science*. 298:389–392.
7. Voss-Foucart, M.-F., M.-T. Fonze-Vignaux, and C. Jeuniaux. 1973. Systematic characters of some polychaetes (Annelida) at the level of the chemical composition of the jaws. *Biochem. System.* 1:119–122.

8. Bhushan, B. 1999. Principles and Applications of Tribology. John Wiley & Sons, New York.

9. Pontin, M. G., D. N. Moses, J. H. Waite, and F. W. Zok. 2007. A nonmineralized approach to abrasion-resistant biomaterials. *Proc. Natl. Acad. Sci. USA.* 104:13559–13564.

10. Oliver, W. C., and G. M. Pharr. 1992. An improved technique for determining hardness and elastic modulus using load and displacement sensing indentation experiments. *J. Mater. Res.* 7:1564–1583.

11. Liu, Y., L. Hong, V. R. Kempf, K. Wakamatsu, S. Ito, and J. D. Simon. 2004. Ion-exchange and adsorption of Fe(III) by *Sepia* melanin. *Pigment Cell Res.* 17:262–269.

12. Zheng, J., Z. R. Zhou, J. Zhang, H. Li, and H. Y. Yu. 2003. On the friction and wear behaviour of human tooth enamel and dentin. *Wear.* 255:967–984.

13. Zaslansky, P., A. A. Friesem, and S. Weiner. 2006. Structure and mechanical properties of the soft zone separating bulk dentin and enamel in crowns of human teeth: insight into tooth function. *J. Struct. Biol.* 153:188–199.

14. Tesch, W., N. Eidelman, P. Roschger, F. Goldenberg, K. Klaushofer, and P. Fratzl. 2001. Graded microstructure and mechanical properties of human crown dentin. *Calcif. Tissue Int.* 69:147–157.

15. Ho, S. P., M. Balooch, H. E. Goodis, G. W. Marshall, and S. J. Marshall. 2004. Ultrastructure and nanomechanical properties of cementum dentin junction. *J. Biomed. Mater. Res. A.* 68A:343–351.

16. Zizak, I., P. Roschger, O. Paris, B. M. Misof, A. Berzlanovich, S. Bernstorff, H. Amenitsch, K. Klaushofer, and P. Fratzl. 2003. Characteristics of mineral particles in the human bone/cartilage interface. *J. Struct. Biol.* 141:208–217.

17. Gupta, H. S., S. Schratter, W. Tesch, P. Roschger, A. Berzlanovich, T. Schoeberl, K. Klaushofer, and P. Fratzl. 2005. Two different correlations between nanoindentation modulus and mineral content in the bone-cartilage interface. *J. Struct. Biol.* 149:138–148.

18. Waite, J. H., H. C. Lichtenegger, G. D. Stucky, and P. Hansma. 2004. Exploring molecular and mechanical gradients in structural bioscaffolds. *Biochemistry.* 43:7653–7662.

19. Schofield, R. M. S., M. H. Nesson, and K. A. Richardson. 2002. Tooth hardness increases with zinc-content in mandibles of young adult leafcutter ants. *Naturwissenschaften.* 89:579–583.

20. Schöberl, T., and I. L. Jager. 2006. Wet or dry—hardness, stiffness, and wear resistance of biological materials on the micron scale. *Adv. Eng. Mater.* 8:1164–1169.

21. Wang, R. Z., L. Addadi, and S. Weiner. 1997. Design strategies of sea urchin teeth: structure, composition and micromechanical relations to function. *Philos. Trans. R. Soc. Lond. B Biol. Sci.* 352:469–480.

22. Hornbogen, E. 1986. Friction and wear of materials with heterogeneous microstructures. *In* Friction and Wear of Polymer Composites. K. Friedrich, editor. Elsevier, New York. 61–88.

23. Sole, B. M., and A. Ball. 1996. On the abrasive wear behaviour of mineral filled polypropylene. *Tribol. Int.* 29:457–465.

24. Kukureka, S. N., C. J. Hooke, M. Rao, P. Liao, and Y. K. Chen. 1999. The effect of fibre reinforcement on the friction and wear of polyamide 66 under dry rolling-sliding contact. *Tribol. Int.* 32:107–116.